

Time evolution of the distribution function for stochastically heated relativistic electrons in a laser field of picosecond duration

L.A. Borisenko, N.G. Borisenko, Yu.A. Mikhailov,
A.S. Orekhov, G.V. Sklizkov, A.M. Chekmarev, A.A. Shapkin

Abstract. We report a numerical analysis of the stochastic acceleration of electrons, stipulated by a random change in the phase of the force acting on the electron. The main source of randomness is the random spatial distribution of electromagnetic fields in the focal region of multimode laser radiation. A typical frequency of the random phase change corresponding to the maximum impact of the effect under consideration lies in the range of $(0.25–0.5)\nu$ (ν is the radiation frequency of a neodymium laser). A wave packet model convenient for calculations taking into account the radiative transitions of the neodymium ion is proposed. The dependence of the average energy of relativistic electrons on the flux density in the range of $10^{15}–10^{18}$ W cm⁻² is calculated. The time dependence of the average electron energy during the laser pulse in the form of approximating formulas is constructed. The typical time for the development of stochastic heating of electrons is determined. It is found that the stochastic acceleration process weakly depends on the laser pulse duration, when the latter exceeds several hundred periods of the electromagnetic wave.

Keywords: laser plasma, stochastic heating of electrons, electron distribution function.

1. Introduction

Recently, in many studies on the irradiation of solid targets by high-intensity laser radiation, the generation of electrons with an anomalously high energy being significantly higher than the equilibrium energy for the relevant flux density has been observed both experimentally and theoretically (see, e.g., [1–5]). Interest in the studies on the generation of high-energy electrons in laser plasma is stipulated not only by the importance of this process for laser thermonuclear fusion, but also by the urgency of using such electrons for the diagnostics of plasma and other objects, and also for solving the fundamental problems of correct derivation of the matter state equation under extreme conditions and, accordingly, for constructing the behaviour models for dense and super-dense plasma at high temperatures [3, 6, 7]. In experiments on the Doppler shift of resonant lines of multiply charged ions in the X-ray range, Basov et al. [8] for the first time observed the ion velocities corresponding to an anomalously high energy (sev-

eral megaelectronvolts) at moderate intensities on the target ($\sim 10^{13}$ W cm⁻²). Generation of strongly ionised ions with anomalously high energies under resonance absorption conditions was also observed and explained for longer wavelength radiation of the CO₂ laser [9]. The presence of these ions also indicates the generation of high-energy electrons. One of the explanations for the appearance of such electrons may be the stochastic mechanism of heating of charged particles in an electromagnetic field with a random change in the field phase, and, consequently, in the force acting on the electron in the course of its motion [6, 10, 11]. Generation of high-energy electrons also took place in hydrodynamic calculations, including the interpretation of some experiments [7]. As shown by recent experiments [12], heating of electrons up to relativistic temperatures makes it possible to use laser plasma as a point source of positrons and, in the long run, to form electron–positron plasma.

In a free electromagnetic field of a light wave, the electron is periodically accelerated and decelerated, thus oscillating in the energy space and gaining on average some oscillation energy comparable to the energy acquired per quarter of the wave period. This energy is not much larger than the Maxwellian (thermal) energy in the laser plasma. Periodic electron energy variations occur much more slowly than the variations of the wave amplitude, at least for the particle relativistic motion in the fields with flux densities of more than 10^{13} W cm⁻². If, at the end of the acceleration period, the local wave phase and, correspondingly, the phase of the Lorentz force acting on the electron are changed, a possibility of multifold acceleration appears. In an ideal case, it is desirable to change the phase synchronously with the electron motion. In reality, the change in the wave phase that an electron ‘sees’ occurs randomly. The sources of randomness may be the electromagnetic field fluctuations caused by the spatially inhomogeneous structure of multimode radiation focused on the target [5, 13]; the field distortions stipulated by the oscillations arising in the plasma, which leads to the emergence of spontaneous electric fields in the longitudinal direction [10, 11]; the fluctuations of the relative phase of spectral components of the inhomogeneously broadened line of laser radiation; the spontaneous magnetic field [14]; and the fluctuations in the plasma refractive index when using low-density microstructured targets [15].

By measuring directly the emission current, the authors of Refs [2, 3] experimentally recorded electrons with an anomalously high energy as compared with the thermal energy. It was found that a significant fraction ($\sim 10\%$) of electrons have an energy over 100 keV with a luminous flux density of $\sim 10^{13}–10^{14}$ W cm⁻², which corresponds to a plasma temperature of ~ 500 eV. Thus, the fraction of such electrons turns

L.A. Borisenko, N.G. Borisenko, Yu.A. Mikhailov, A.S. Orekhov, G.V. Sklizkov, A.M. Chekmarev, A.A. Shapkin P.N. Lebedev Physical Institute, Russian Academy of Sciences, Leninsky prosp. 53, 119991 Moscow, Russia, e-mail: sklizkov@sci.lebedev.ru

Received 12 May 2017; revision received 18 July 2017
Kvantovaya Elektronika 47 (10) 915–921 (2017)
Translated by M.A. Monastyrskiy

out to be much larger than it should be for the Maxwellian distribution. An attempt was made in works [5, 6] to evaluate numerically the possibility of stochastic heating of the electron gas in the electromagnetic field of laser radiation and to present a qualitative comparison with experimental results. In this case, the electron gas temperature is estimated as the average energy with respect to the relevant nonequilibrium distribution function for relativistic electrons, averaged over the laser pulse duration.

In the present work we consider the dynamics of electron emission as a function of the laser pulse structure which is represented in the form of a wave packet corresponding to the spectral composition of the radiation of a neodymium laser. Emission of electrons in this case is understood as their escape from the region of interaction with the electromagnetic field, i.e. from the region of laser radiation focusing onto the target. The flux distribution function of emitted electrons is of interest. The shape of the distribution function is determined both in energy and momentum representations. The time dependence of the distribution function is found during the laser pulse action at a radiation intensity up to 10^{18} W cm⁻². Formulas for electromagnetic fields are obtained with allowance for the random parameters determining the stochastic acceleration of the particles. Probable sources of randomness in a laser–plasma system are analysed.

2. A wave packet simulating the laser field in the interaction region

The radiation line structure of the neodymium laser with inhomogeneous broadening of the Stark components in the neodymium transition ${}^4F_{3/2} - {}^4I_{11/2}$ and the processes of generation of short laser pulses in neodymium glass have been studied in detail [16–18]. Based on the data on the neodymium laser, we construct an analytical model of a short laser pulse (wave packet), which is convenient for numerical calculations.

Consider a number of assumptions underlying this model. In contrast to work [16], two upper Stark sublevels and six lower sublevels are considered equidistant, and their splittings are the same, although in reality the upper level splitting is almost two times greater than the distance between the sublevels of the lower level ${}^4I_{11/2}$ (75 cm⁻¹). Twelve Stark components in our model have the same frequency form, close to the Lorentzian one, but different amplitudes.

A short laser pulse has a bell-like parabolic shape, i.e., an ideal contrast. In the near zone (at the laser output), the field intensity in the beam has a near-rectangular super-Gaussian (of eighth degree) distribution over the aperture with a sharp dip at the edges. Thus, the wavefront field is inhomogeneous, and the field amplitude variation is random. The field amplitude fluctuations along the aperture constitute $\sim 10\%$, and, accordingly, the field's local phase varies randomly. The spatial distribution of intensity over the laser beam aperture has the form of a speckle structure. The spatial inhomogeneity size of the amplitude and phase is of the order of several millimetres (spatial coherence), which corresponds to that experimentally observed for neodymium lasers. Thus, the wave front curvature before entering the focusing system locally changes in a random manner. All this has an impact on the electromagnetic field distribution in the focusing region. Note that in a target with a subcritical density characterised by bulk absorption, the interaction of laser radiation with elec-

trons occurs in the focusing region volume inside a low-density medium rather than on the surface.

Next, to simulate a random structure of an electromagnetic field in the focal region, we define a wave packet with random phase parameters, as described below.

Let the amplitudes of the Stark components decrease symmetrically with distance from the centre frequency, in contrast to the numerical calculations of the above-mentioned works. In our model, the effects associated with cross-relaxation and the efficiency of the inversion reset are not taken into account. All 12 Stark components of the radiation line are assumed equivalent.

The formulas

$$f_i = \left(1 - \frac{t_i}{\tau}\right) \frac{t_i}{\tau}, \quad f(j) = \left(1 - \frac{j}{N_L}\right) \frac{j}{N_L}$$

define, respectively, the temporal shape of a pulse having a duration τ and the distribution of the components over the field amplitude. Here the subscript i is the current temporal index ranging from 1 to $N = n_\lambda N_p$; n_λ is the number of wave periods; N_p is the number of points per period; N_L is the number of components in a line; and j is the number of the laser line component. In this case, we can represent the expression for the composite wave with in-phase components in the form

$$E_i = \sum_j \left\{ f(j) f_i \exp \left[i \omega_0 \left[1 + \frac{\Delta n_\lambda}{n_\lambda} \left(j - \frac{N_L}{2} \right) \right] \left(t_i - \frac{\tau}{2} \right) \right] \right\},$$

where ω_0 is the centre frequency; and Δn_λ is the number of periods corresponding to the frequency interval between neighbouring equidistant components.

A wave with random component phases appears as

$$E_{\text{Rnd}}(j, t) = \sum_j [f_e(j, t) f_i],$$

where

$$f_e(j, t) = f(j) \exp \left\{ i \left[\omega_0 \left[1 + \frac{\Delta n_\lambda}{n_\lambda} \left(j - \frac{N_L}{2} \right) \right] \left(t_i - \frac{\tau}{2} \right) - \Phi_j \right] \right\};$$

and $\Phi_j(t)$ are the random phases of the components relative to each other within the uncertainty relation.

The expressions for the total field amplitude of all components with a phase ψ_i external to the wave packet have the form

$$E_{\text{Rnd}\psi}(t) = \left\{ \sum_j [f_e(j, t) f_i] \right\} \exp(i\psi_i).$$

A few words should be said about the random function ψ_i . The phase ψ_i corresponds to the field phase that an electron 'sees'. It is determined by the relative position of the electron and the wave. In other words, this is a local field phase at the location of a moving electron at a given time. This phase depends on the spatial structure of the field, since the electron, being as a rule relativistic, in some measure moves in space randomly, changing, along with its position, also its momentum, both in magnitude and direction. The process of interaction of an electron with a field in this case occurs for a sufficiently long time, i.e., during many (tens and hundreds) periods. This is the so-called stochastic acceleration, in contrast to direct acceleration which lasts a single period or sev-

eral periods in the case several independent lasers are used. Therefore, in our case, the random phase variation in time is also essential. We should note that the electric field is responsible for electron acceleration, while the magnetic field is responsible for changing its trajectory, including the change in the direction of its momentum. This is equivalent to a random variation of the electromagnetic field phase ψ_i in time at the electron location. Thus, this time-dependent function, in fact, simulates the random nature of the force acting on the electron along its trajectory.

Figure 1 shows an instantaneous phase picture of the laser radiation components at a certain time moment. The phase of each component changes with time independently. A random change in the phase of the field of each component is assumed pre-determined, i.e. it does not depend on the state of the ensemble of electrons. The envelope of the field maxima of the components has a bell-like shape.

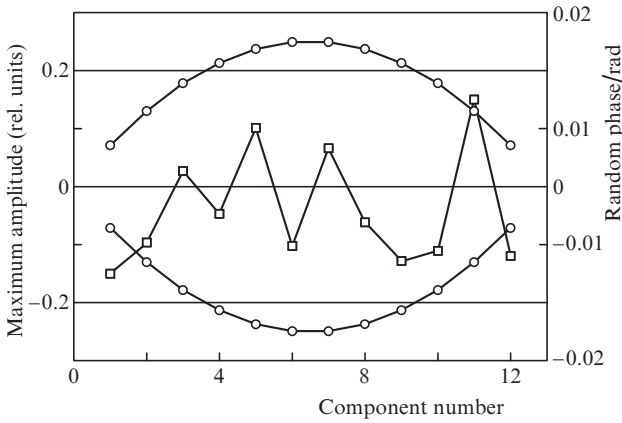


Figure 1. Instantaneous phase picture of components at a given time moment: (o) maximum amplitudes of components and (□) random phases of each component.

A model of the spectral line structure for the neodymium laser on silicate glass with a radiation wavelength $\lambda = 1.06 \mu\text{m}$ is illustrated in Fig. 2. It shows the frequency dependence of the wave's electric field strength. The black thick curve cor-

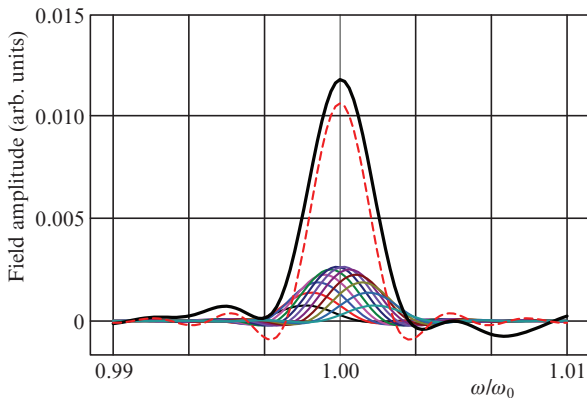


Figure 2. (Colour online) Laser line structure with random phases consisting of 12 components (black thick curve). The family of thin curves is the line of 12 components. The dashed curve is a composite line without taking into account the random phase ψ_i .

responds to the instantaneous line shape, taking into account the random phases of all the components and the function ψ_i . The asymmetry (both phase and amplitude) of the line's wings with respect to the centre frequency $\omega_0 = 1.78 \times 10^{15} \text{ s}^{-1}$ can be observed. A small frequency variation at the maximum also occurs (not shown in Fig. 2). For comparison, the line's field is shown with no allowance for the perturbing phases for 12 components (dashed curve). Here a complete symmetry of the wings is observed. All the curves have been obtained for a pulse duration of 3.5 ps, i.e., for as many as $\sim 10^3$ periods of the field oscillations.

3. The motion equations with random parameters

The motion equations for a relativistic electron can be written in the form:

$$\frac{d\mathbf{p}(\mathbf{r}, t)}{dt} = \frac{q\mathbf{p}(\mathbf{r}, t) \times \mathbf{B}(\mathbf{r}, t)}{\sqrt{1+p^2}} + q\mathbf{E}(\mathbf{r}, t) - \mathbf{L}(\mathbf{p}),$$

$$\mathbf{r}(t) = \int_0^t \frac{\mathbf{p}(\mathbf{r}, t)}{\sqrt{1+p^2}} dt, \quad T_{\text{kin}} = \sqrt{1+p^2} - 1,$$

where $t = ct'$ (in cm);

$$\mathbf{p} = \frac{\mathbf{p}'c}{mc^2} \quad (|\mathbf{p}| = \sqrt{\gamma^2 - 1}), \quad T_{\text{kin}} = \frac{T'_{\text{kin}}}{mc^2},$$

$$\mathbf{E}(\mathbf{r}, t) = \frac{q\mathbf{E}'(\mathbf{r}, t)}{mc^2}, \quad \mathbf{B}(\mathbf{r}, t) = \frac{q\mathbf{B}'(\mathbf{r}, t)}{mc^2}$$

are the reduced momentum, electron kinetic energy, electric and magnetic fields, respectively; q is the electron charge; m is its mass at rest; and γ is the relativistic factor. In the formulas of this section, the quantities with a prime are real physical variables. The last term $\mathbf{L}(\mathbf{p})$ in the first equation takes into account the deceleration force $f_{\text{rad}} = |dp_{\text{rad}}/dt|$ acting on the accelerated particle at the expense of the electron radiation response in the electromagnetic wave field, and also the deceleration force $f_{\text{ee}} = |dp_{\text{ee}}/dt|$ resulting from the long-range interaction of a relativistic electron with a cloud of relatively slow electrons with a concentration $n \approx 1.6 \times 10^{20} \text{ cm}^{-3}$. Thus, the deceleration force is $L(\mathbf{p}) = f_{\text{rad}} + f_{\text{ee}}$, and its direction coincides with the direction \mathbf{p} of the momentum of the accelerated electron. The excitation of electron plasma waves by a bunch of accelerated electrons is not taken into account.

To evaluate the radiation response, we use the expression

$$\left| \frac{d\epsilon'}{dt'} \right| = \frac{2q^4 B'^2 p'^2}{3m^4 c^5}$$

for the energy loss ϵ' of a relativistic electron due to magnetic-bremsstrahlung in the field of a plane polarised wave [19].

In our notations, we obtain a relation for the radiation force

$$\left| \frac{dp_{\text{rad}}}{dt} \right| = \frac{1}{mc^2} \left| \frac{dp'_{\text{rad}}}{dt'} \right|$$

$$= \frac{\sqrt{1+p^2}}{mc^3 p} \left| \frac{d\epsilon'}{dt'} \right| = \frac{2}{3} r_0 B^2 p \sqrt{1+p^2},$$

where r_0 is the classical radius of the electron. We should note that although the radiation response force increases strongly with increasing electron energy, it is still substantially less than the accelerating force for the range of the laser flux densities under consideration.

The deceleration force of particles due to the long-range interaction is determined for the case of Coulomb scattering of a relativistic electron by small angles on relatively resting electrons [20]. As the maximum impact parameter, we take the Debye radius r_D , and as the minimum impact one – the Compton wavelength r_C . The energy loss per unit length x is given by the expression

$$\frac{d\varepsilon'}{dx} = 4\pi r_0^2 \frac{m^3 c^6 \gamma^4}{(p'c)^2} \ln \frac{r_D}{r_C}.$$

Hence the deceleration force is

$$\left| \frac{dp_{ee}}{dt} \right| = 4\pi n r_0^2 \frac{(1+p^2)^2}{p^2} \ln \frac{r_D}{r_C}.$$

In the calculations, the Coulomb logarithm is assumed equal to ~ 10 .

In our case, the electromagnetic field is assumed strong and pre-determined, so that the energy dissipation due to the excitation of plasma oscillations and their damping is not considered. These equations do not take into account the losses caused by bremsstrahlung resulting from collisions with ions. However, it should be noted that at flux densities above $10^{18} \text{ W cm}^{-2}$, the radiation response at each step (cell) becomes significant and must be taken into account in electron trajectory calculations.

Making allowance for the friction forces $L(p)$ leads to a slight ‘dip’ in the high-energy part of the distribution function, which virtually does not affect the average energy evolution. The Coulomb force f_{ee} does not explicitly depend on the intensity; therefore, its contribution to electron deceleration decreases with increasing field amplitude. As for the radiation response, the situation here is opposite. When the field amplitude increases, the force f_{rad} of magnetic bremsstrahlung response quadratically increases. In the relativistic case, the ratio of the radiation force and the ponderomotive force F_{em} appears as

$$\eta = \frac{f_{rad}}{F_{em}} \approx \frac{4r_0 B p^2 \sqrt{1+p^2}}{3} \propto I_L^{1.7},$$

where, as follows from the calculations, $p \propto \gamma \propto I_L^{0.4}$. For example, at a laser radiation flux density of $I_L \approx 10^{18} \text{ W cm}^{-2}$, $\eta \approx 10^{-3}$, while at $I_L \approx 2 \times 10^{19} \text{ W cm}^{-2}$ it can reach ~ 0.16 . The above expression for the ratio of forces is only valid for $\eta \ll 1$.

The electromagnetic field is assumed to be specified, i.e., independent of the plasma properties. Based on the said above, we can write the expressions for the electric and magnetic fields with random phases under consideration in the form:

$$\begin{aligned} \mathbf{E}(\mathbf{r}, t) &= \mathbf{E}_0(\mathbf{r}) E_{Rnd\psi}(t) \exp(ik_0 t) \\ &\times [(1 - \gamma_r) \exp(-\mathbf{k}\mathbf{r}) + 2\gamma_r \cos(\mathbf{k}\mathbf{r} + \phi(\mathbf{r}))], \end{aligned}$$

$$\mathbf{B}(\mathbf{r}, t) = \mathbf{B}_0(\mathbf{r}) E_{Rnd\psi}(t) \exp(ik_0 t) \times$$

$$\times [(1 - \gamma_r) \exp(-\mathbf{k}\mathbf{r}) + \exp(-i\pi/2) 2\gamma_r \sin(\mathbf{k}\mathbf{r} + \phi(\mathbf{r}))].$$

Here γ_r is the amplitude reflection coefficient; \mathbf{k} is the wave number; $k_0 = \omega_0/c$; and $\phi(\mathbf{r})$ is the random phase of the reflected wave. The reflected wave is formed in the region of critical density. In our model, it is assumed that the reflected wave has the same phase structure as that of the incident wave. This assumption is justified only for small reflection coefficients (in the calculations it is assumed that $\gamma_r = 0.2$) which are realised in the majority of experiments on laser plasma heating. The motion of electrons was considered from a certain restricted region of space with a random location of electrons, similarly to [6]. The initial particle distribution in the momenta was chosen Maxwellian, with a temperature of about 1 keV, which corresponds to the plasma corona temperature near the critical density region. As a result of the angular distribution of modes in the laser beam far zone that corresponds to the radiation focusing region, speckle structures are formed in the field distribution, and the changes in the phase of the field acting on the electron are random when passing from one peak to another [5]. This leads to the fact that the moving electron is subjected to the electromagnetic field with a phase that changes greatly during a time being much shorter than the wave period (i.e., in discrete steps). In this case, the phase is considered constant in the interval between jumps. The random distribution of the relative phase is taken into account for each spectral component, and the frequency of the field phase change corresponds to 0.4ν (ν is the laser radiation frequency). The motion equations were solved by the fourth-order Runge–Kutta method with adaptive step and the spatial resolution in the calculations was 50 points per electromagnetic wave period. To find the time evolution of the electron distribution function along with the mean energy T of electrons, we used $\sim 10^4$ test particles. The statistical accuracy of determining the electron energy T averaged over the entire particle ensemble at a given time moment constitutes $\sim 1\%$.

4. Results of calculations and their discussion

Typical particle trajectories in the process of acceleration without taking friction forces into account in the motion equations are given in [5]. Since the friction forces are small, they have little impact on the size of the acceleration region. At the initial stage, most electrons are captured into the acceleration regime. Acceleration mainly occurs along the wave vector. In our case, the electron beam divergence at the pulse end was ~ 0.05 rad with a flux density of $10^{18} \text{ W cm}^{-2}$. In this range of radiation flux densities, the electron beam divergence decreases proportionally to $T^{-1/2}$.

Proceeding from the results of work [5] and our calculations, the size of the interaction region (the typical size of trajectories) turns out equal to ~ 0.05 cm in the longitudinal direction, and ~ 0.01 cm in the transverse direction. In our calculations, the plasma density is considered constant in this region. At the end of the laser pulse, all the particles move by inertia, no longer interacting with the electromagnetic field and plasma. We should note that the dependence of energy on time for each particle has a very non-smooth random character; the energy jumps are sometimes comparable to the energy itself. The same applies to the phase dependences and, to a lesser extent, to the dependences of coordinates on time. However, averaging over the ensemble of particles gives a relatively smooth dependence $T(t)$. (The average energy T is

not the electron temperature; it rather represents a spread in energy of electrons in the directed beam.)

The results of calculating the time evolution of the normalised probability density distribution of electrons are shown in Fig. 3. The curves here are presented for different time moments during the laser pulse action. The distribution function undergoes a significant change in the course ~ 100 laser wave periods after switching the field on (first five curves, starting from the left). The distribution function maximum at the end of the laser pulse can sometimes slightly shift towards lower energies. At the same time, the average electron energy continuously increases with time and reaches a maximum value at the end of the laser pulse. This can be explained by the fact that, by the end of the laser pulse, the distribution function tail is always located in the region of higher energies. After 2.5 ps (~ 700 periods), the distribution function experiences saturation, and its shape remains further virtually unchanged (three curves shown by thin lines). The fine-scale random structure that most clearly manifests itself at the end of of the laser pulse is not related to the accuracy of the calculations. It is a consequence of the stochastic nature of the spatiotemporal structure of the electromagnetic field. A change in the distribution function within the high-energy region occurs at the leading edge of the laser pulse, while the energy distribution of electrons remains virtually unchanged in the region of the pulse decay. The distribution of electrons in energies is very different from the Maxwellian one, especially in its high-energy part.

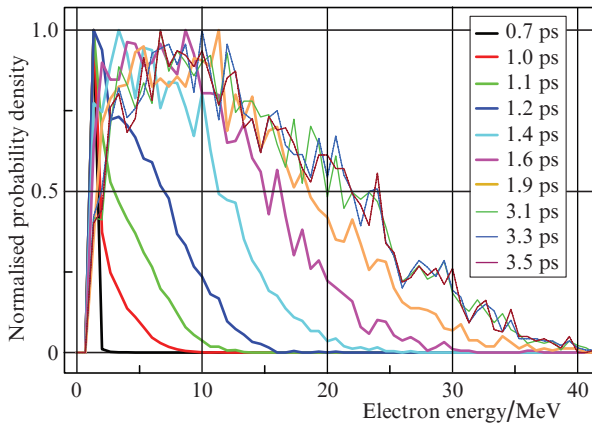


Figure 3. (Colour online) Time evolution of the probability density distribution of electrons, normalised to its maximum.

The average energy of electrons at a given time moment was calculated over the entire ensemble of relativistic electrons, regardless of their location by this time moment. The calculated values of the mean energy T versus time are shown in Fig. 4 (curve with circles). The laser pulse shape was chosen to be bell-like, which is closer to real pulses of neodymium lasers compared to rectangular or triangular pulses.

The maximum energy growth rate is observed at the leading edge of the pulse, where the time derivative of the local field amplitude is positive. The initial stage of energy accumulation by an electron is described by the power-law dependence $T_{\text{in}} \propto \mu^\beta$ (dashed curve), where μ is the number of cells in which the force phase changes. That number is approximately equal to half the number of field periods in the laboratory coordinate system by the given time moment. The time

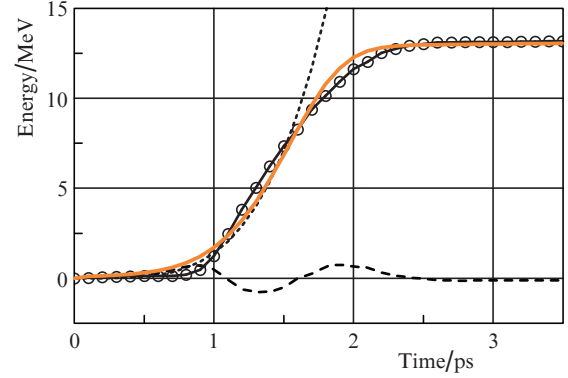


Figure 4. Time dependence of the average electron energy $T(t)$ (a curve with circles; the circle size characterises the statistical accuracy of kinetic energy calculation). The grey curve is an approximation by the formula for $T_{\text{app}}(t)$. The dashed curve is the power-law time dependence $T_{\text{in}}(t)$ of the electron energy at the leading edge of the bell-shaped laser pulse. The dashed curve shows the deviation of the approximation values $T_{\text{app}}(t)$ from the calculated values $T(t)$.

dependence of the kinetic energy averaged over the entire ensemble of electrons can be analytically represented in the form

$$T_{\text{in}}(t) = B_{\text{in}} t^\beta,$$

where energy is taken in MeV and time in ps; the coefficient B_{in} weakly depends on the field intensity in the relativistic case and is equal to ~ 1.4 in the flux density range of $10^{17} - 10^{18} \text{ W cm}^{-2}$; and the stochastic electron acceleration index $\beta \approx 4$. This formula is valid at the leading edge of the laser pulse for a time less than 1.5 ps, which is less than 400 periods. The corresponding dependence of $T_{\text{in}}(t)$ is presented in Fig. 4 by the dashed curve.

During the pulse, the energy growth slows down, and after ~ 700 periods (~ 2.5 ps) becomes saturated. Based on the calculations, we describe the energy evolution (in MeV) during the laser pulse action by the approximate analytical expression with two empirical parameters B_1 and B_2 :

$$T_{\text{app}}(t) = B_0 \left[\frac{1}{1 + \exp(-B_1 t^\alpha)} + B_2 \sqrt{t} - 0.5 \right].$$

Here time is measured in picoseconds; the parameters $B_1 = 0.227$ and $B_2 = 0.012$ are virtually intensity independent in the flux density range of $10^{16} - 10^{18} \text{ W cm}^{-2}$; the parameter B_0 depends on the laser radiation intensity: $B_0 \propto I_L^\alpha$; and the parameter α is determined from the slope of the dependences of the average electron energy on the flux density given in Fig. 5. For curve (*J*) in Fig. 5, the exponent α is about 2/5 in the flux density range $10^{16} - 10^{18} \text{ W cm}^{-2}$. For example, for a flux density of $2 \times 10^{18} \text{ W cm}^{-2}$, the parameter B_0 is about 25 MeV. The dependence of the average electron energy calculated according to the approximation formula for $T_{\text{app}}(t)$ is represented in Fig. 4 by a grey curve. The dashed curve in Fig. 4 illustrates the accuracy in the case of approximation by means of the analytical expression $T_{\text{app}}(t)$ compared to the dependence $T(t)$ obtained numerically. Note that the function $T_{\text{in}}(t)$ represents the first term of the fourth order in the time expansion of the function $T_{\text{app}}(t)$.

At the initial stage, with increasing intensity in time, the stochastic acceleration of electrons, averaged over the entire

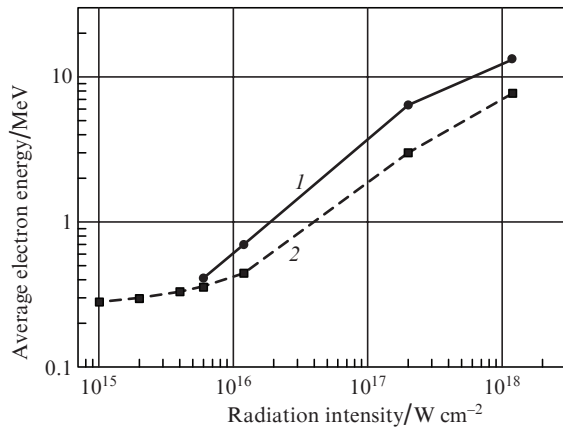


Figure 5. (1) Average electron energy $B_0/2$ by the time moment of laser pulse termination and (2) electron energy averaged over all electrons and heating time as a function of the radiation intensity.

ensemble of particles, resembles in its nature the Fermi acceleration [21] for a relativistic particle in a non-autonomous dynamic system. However, in the middle of the pulse, where the field amplitude varies only slightly, the energy growth rate decreases, and at the pulse end, with the average intensity decreasing with time, the average energy experiences saturation and remains constant (without taking into account the losses caused by bremsstrahlung). The acceleration development after switching on laser radiation occurs during ~ 150 wave-phase perturbations, i.e., during ~ 0.5 ps for a wavelength $\lambda = 1.06 \mu\text{m}$.

In work [7], using the ATLANT-HE software [7], two-dimensional hydrodynamic calculations of the energy of fast electrons being produced during heating of an aluminium target by the iodine laser radiation (first and second harmonic) with an intensity of $\sim 10^{16} \text{ W cm}^{-2}$ were conducted. According to the scaling performed in this work, the dependence of energy on intensity is determined by the expression $T \approx 8(I_L \lambda^2)^{2/3}$, where T is taken in keV, I_L – in PW cm^{-2} and λ – in μm . Estimates according to this formula give $T \approx 40$ keV at flux densities of $\sim 10^{16} \text{ W cm}^{-2}$, which is approximately three times less than the value obtained from the results of the present work. It should also be noted that the scaling performed in the work mentioned above gives a different, as compared with the present work, character of the energy dependence of fast electrons on the flux density of laser radiation on the target in stochastic processes. A different form of the dependences of the average electron energy on the radiation intensity is apparently explained by a difference between the distribution functions of electrons obtained in this work and that used in [7, 22].

A few words should be said about the possibility of experimental observation of the stochastic mechanism of electron acceleration. The necessary experimental conditions can be implemented by irradiating low-density targets [23], when plasma with a homogeneous subcritical electron density is formed over the entire volume of the interaction region, with a transverse size of ~ 0.01 cm and a longitudinal size of ~ 0.05 cm. In this case, the distribution function is measured as a function of the laser pulse duration (in the range 0.2–3 ps), along with the dependence of the average energy at the pulse end on the radiation intensity at the target (up to $\sim 10^{18} \text{ W cm}^{-2}$). This experiment is possible, for example, using such picosecond installations as PICO-2000 LULI

(École Polytechnique, Palaiseau) [24], PHELIX-GSI (Darmstadt) [25], TRIDENT [Los Alamos] [26], OMEGA EP (Rochester) [27], and others.

5. Conclusions

The stochastic mechanism of electron heating we have considered can only develop at the pulse duration of the order of 1 ps or more, including that at nanosecond durations. The average energy of electrons can substantially exceed (by more than an order of magnitude) the energy of oscillatory motion, i.e. the energy of direct acceleration in the laser field. In this case, the length on which acceleration and energy accumulation occur is significantly reduced. The formulas derived from numerical analysis to describe the time dependence of the average energy of electrons can be useful both for hydrodynamic calculations and for experimental data processing.

We also note that stochastic acceleration of relativistic electrons occurs mainly along the wave vector [4, 5, 11]. This is equivalent to the emergence of a longitudinal macroscopic electric field (stochastic ponderomotive force) in the interaction region. Such a mechanism of particle acceleration can be used in studies on magnetic reconnection [28] and in modelling the acceleration of matter in astrophysical objects (bursts of high-energy radiation, cosmic ray acceleration). The same mechanism can also lead to undesirable pre-heating and instabilities in compression of a thermonuclear target.

Acknowledgements. The authors are grateful to S.Yu. Gus'kov, N.N. Demchenko, Yu.V. Senatskii and S.G. Bochkarev for useful discussions, and to A.A. Rupasov for supporting this work.

The work was partially supported by the Russian Foundation for Basic Research (Grant No. 17-02-00366).

References

- Roxusseau C., Amiranoff F., Labaune C., Matthieussent G. *Phys. Fluids B*, **4** (8), 2589 (1992).
- Ivanov V.V., Knyazev A.K., Korneev N.E., Kutsenko A.V., Matsveiko A.A., Mikhailov Yu.A., Osetrov V.P., Popov A.I., Sklizkov G.V., Starodub A.N. *Prib. Tekh. Exp.*, (4), 112 (1995).
- Ivanov V.V., Knyazev A.K., Kutsenko A.V., Matsveiko A.A., Mikhailov Yu.A., Osetrov V.P., Popov A.I., Sklizkov G.V., Starodub A.N. *JETP*, **82** (4), 677 (1996) [*Zh. Eksp. Teor. Fiz.*, **109**, 1257 (1996)].
- Nakamura T., Kato S., Tamimoto M., Kato T. *Phys. Plasmas*, **8** (5), 1801 (2002).
- Mikhailov Yu.A., Nikitina L.A., Sklizkov G.V., Starodub A.N., Zhurovich M.A. *Laser Part. Beams*, **26**, 525 (2008).
- Krylenko Yu.V., Mikhailov Yu.A., Orekhov A.S., Sklizkov G.V., Filippov A.A. *Bull. Lebedev Phys. Inst.*, **37** (10), 324 (2010) [*Kr. Soobshch. Fiz.*, **37** (10), 46 (2010)].
- Gus'kov S.Yu., Demchenko N.N., Kasperczyk A., Pisarczyk T., Kalinowska Z., Chodukowski T., Renner O., Smid M., Krousky E., Pfeifer M., Skala J., Ullschmied J., Pisarczyk P. *Laser Part. Beams*, **32**, 177 (2014).
- Basov N.G., Bobashov S.V., Goetz K., Kalashnikov M.P., Meshcherkin A.P., Mikhailov Yu.A., Rode A.V., Sklizkov G.V., Fedotov S.I., Forster E., Endert H. *JETP Lett.*, **36** (7), 281 (1982) [*Pis'ma Zh. Eksp. Teor. Fiz.*, **36** (7), 229 (1982)].
- Gus'kov S.Yu., Demchenko N.N., Makarov K.N., Rozanov V.B., Satov Yu.A., Sharkov B.Yu. *Quantum Electron.*, **41** (10), 886 (2011) [*Kvantovaya Elektron.*, **41** (10), 886 (2011)].
- Bochkarev S.G., Brantov A.V., Bychenkov V.Yu., Torshin D.V., Kovalev V.F., Baidin G.V., Lykov V.A. *Plasma Phys. Rep.*, **40** (3), 202 (2014).

11. Vais O.E., Bochkarev S.G., Ter-Avetisyan S., Bychenkov V.Yu. *Quantum Electron.*, **47** (1), 38 (2017) [*Kvantovaya Elektron.*, **47** (1), 38 (2017)].
12. Nagel S.R., Meyerhofer D.D., Shepherd R., Hoarty D. *J. Phys. Conf. Ser.*, **688**, 012010 (2016). DOI: 10.1088/1742-6596/688/1/012010.
13. Krylenko Yu.V., Mikhailov Yu.A., Orekhov A.S., Sklizkov G.V., Chekmarev A.M. *J. Russ. Laser Res.*, **32** (1), 19 (2011).
14. Kuzenov V.V., Lebo A.I., Lebo I.G., Ryzhkov S.V. *Fiziko-matematicheskie modeli i metody rascheta vozdeystviya moshchnykh lazernykh i plazmennykh impulsov na kondensirovannye i gazovye sredy* (Physico-Mathematical Models and Methods for Calculating The Effect of High-Power Laser and Plasma Pulses on Condensed and Gaseous Media) (Moscow: MGTU im. Baumana, 2015).
15. Chaurasia S., Leshma P., Murali C.G., Borisenko N.G., Munda D.S., Orekhov A., Gromov A.I., Merkuliev Yu.A., Dhareshwar L.J. *Opt. Commun.*, **343**, 1 (2015). DOI: 10.1016/j.optcom.2015.01.001.
16. Ivanov V.V., Senatskii Yu.V., Sklizkov G.V. *Sov. J. Quantum Electron.*, **16** (3), 422 (1986) [*Kvantovaya Elektron.*, **13** (3), 647 (1986)].
17. Ivanov V.V., Senatskii Yu.V., Sklizkov G.V. *Trudy FIAN*, **178**, 130 (1987).
18. Senatskii Yu.V. *Doct. Thesis* (Moscow: FIAN, 2015).
19. Landau L.D., Lifshitz E.M. *The Classical Theory of Fields* (New York: Pergamon Press, 1971) ch. IX.
20. Lifshitz E.M., Pitaevskii L.P. *Physical Kinetics* (Oxford, New York: Pergamon Press, 1981; Moscow: Science, 1979) Ch. IV.
21. Lichtenberg A.J., Lieberman M.A. *Regular and Stochastic Motion* (New York: Springer, 1983; Moscow: Mir, 1984).
22. Gus'kov S.Yu. *Fiz. Plasmy*, **39** (1), 3 (2013).
23. Casner A., Masse L., Delorme B., Martinez D., Huser G., Galmiche D., Liberatore S., Igumenshchev I., Olazabal M., Nicolai P., et al. *Phys. Plasmas*, **21**, 122702 (2014).
24. Goyon C., Depierreux S., Yahia V., Loisel G., Baccou C., Courvoisier C., Borisenko N.G., Orekhov A.S., Rosmej O., Labaune C. *Phys. Rev. Lett.*, **111**, 235006 (2013).
25. Bagnoud V., Hornung J., Schlegel T., Zielbauer B., Brabetz C., Roth M., Hilz P., Haug M., Schreiber J., Wagner F. *Phys. Rev. Lett.*, **118**, 255003 (2017).
26. Roth M., Bedacht S., Busold S., Deppert O., Schaumann G., Wagner F., et al. *Proc. IPAC-2014* (Dresden, Germany, 2014) WEXB01.
27. Willingale L., Thomas A.G.R., Nilson P.M., Chen H., Cobble J., Craxton R.S., Maksimchuk A., et al. *New J. Phys.*, **15**, 025023 (2013).
28. Gu Y.J., Yu Q., Klimo O., Esirkepov T.Zh., Bulanov S.V., Weber S., Korn G. *High Power Laser Science and Engineering*, **4**, e19 (2016). DOI: 10.1017/hpl.2016.16.